AD-A097 749 CINCINNATI UNIV OH DEPT OF MECHANICAL AND INDUSTRIAL--ETC F/G 2/1
VALIDATION OF FINITE SEGMENT CABLE MODELS.(U)
APR 81 R L HUSTON, J W KAMMAN N00014-76-C-013
UNCLASSIFIED UC-MIE-041581-11-ONR NL

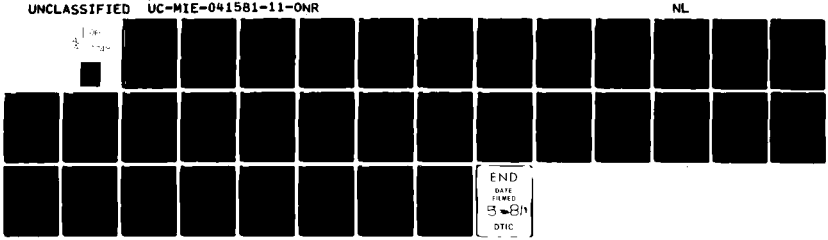

SECURITY CLASSIFICATION OF THIS PAGE (When Data Entered)

(14) REPORT DOCUMENTATION PAGE

READ INSTRUCTIONS BEFORE COMPLETING FORM

1. REPORT NUMBER: ONR-UC-MIE-4[illegible]81-11-ONR	2. GOVT ACCESSION NO. AD-A097749
3. RECIPIENT'S CATALOG NUMBER	
4. TITLE (and Subtitle): (6) VALIDATION OF FINITE SEGMENT CABLE MODELS .	5. TYPE OF REPORT & PERIOD COVERED: (9) Technical rept. 1 Oct 79-15 Apr 81
	6. PERFORMING ORG. REPORT NUMBER
7. AUTHOR(s): (10) Ronald L. Huston, James W. Kamman	8. CONTRACT OR GRANT NUMBER(s): (15) N00014-76-C-0139
9. PERFORMING ORGANIZATION NAME AND ADDRESS: Mechanical & Industrial Engineering, University of Cincinnati, Cincinnati, Ohio 45221 (11) 15 Apr 81	10. PROGRAM ELEMENT, PROJECT, TASK AREA & WORK UNIT NUMBERS: 122303
11. CONTROLLING OFFICE NAME AND ADDRESS: ONR Resident Research Representative, Ohio State University, 1314 Kenner Rd., Columbus, OH 43212	12. REPORT DATE: 4/15/81
	13. NUMBER OF PAGES: 31
14. MONITORING AGENCY NAME & ADDRESS(if different from Controlling Office): Office of Naval Research, Structural Mechanics, Department of the Navy, Arlington, VA 22217 (12) 34	15. SECURITY CLASS. (of this report): Unclassified
	15a. DECLASSIFICATION/DOWNGRADING SCHEDULE

16. DISTRIBUTION STATEMENT (of this Report)

Distribution of this report is unlimited.

17. DISTRIBUTION STATEMENT (of the abstract entered in Block 20, if different from Report)

18. SUPPLEMENTARY NOTES

19. KEY WORDS (Continue on reverse side if necessary and identify by block number)

Cable Dynamics, Model Validation, Chain Systems, Finite-Segment Modelling, Fluid Dynamics Modelling

20. ABSTRACT (Continue on reverse side if necessary and identify by block number)

Analytical and experimental data is presented validating a finite segment cable model. The model consists of a series of pin-connected rigid rods which may have different lengths, diameters, and masses. The model is capable of simulating large, three-dimensional motion of flexible cables. Its principal areas of application are expected to be with the simulation of long, heavy, towing and hoisting cables.

DD FORM 1 JAN 73 1473 EDITION OF 1 NOV 65 IS OBSOLETE S/N 0102-014-6601

Unclassified

SECURITY CLASSIFICATION OF THIS PAGE (When Data Entered)

VALIDATION OF FINITE SEGMENT CABLE MODELS

Ronald L. Huston

and

James W. Kamman

Department of Mechanical and
Industrial Engineering
Mail Location No. 72
University of Cincinnati
Cincinnati, Ohio 45221

This Technical Report was prepared with support of

Office of Naval Research

Contract N00014-76C-0139

A B S T R A C T

Analytical and experimental data is presented validating a finite segment cable model. The model consists of a series of pin-connected rigid rods which may have different lengths, diameters, and masses. The model is capable of simulating large, three-dimensional motion of flexible cables. Its principal areas of application are expected to be with the simulation of long, heavy, towing and hoisting cables.

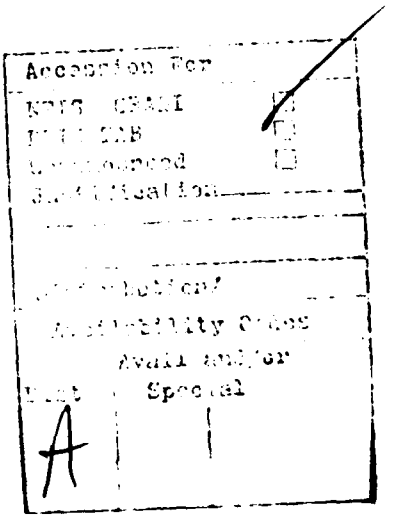

INTRODUCTION

Approximately five years ago we introduced a three-dimensional dynamic finite segment model for cables and chains [1].* The model consists of a series of pin-connected rods or links. The model is developed so that arbitrary external forces may be exerted on the links. The dynamics of the system is then determined through numerical integration of the governing equations of motion. In this report we present data which validates analytical predictions of the model.

Figure 1. shows a schematic representation of the model. The number of links N is arbitrary. The length, diameter, mass, and inertias of the individual links may also be arbitrarily chosen. This model is expected to be effective in studying the nonlinear, three-dimensional, dynamic behavior of long, heavy cables [1,2]. Particular application with submerged towing cables has also been suggested [3].

The attractive features of the model are: 1) the arbitrary dimensions and physical parameters of the links of the model; 2) the arbitrary specification of externally applied forces; 3) the use of relative orientation angles between the links to define the system configuration; and 4) the use of Lagrange's form of d'Alembert's principle to develop the governing equations of motion. The use of relative orientation angles is a convenience in the specification of the system's configuration and in the introduction of

---

* Numbers in brackets refer to References at the end of the report.

flexible and/or torsional springs and dampers between the links. Lagrange's form of d'Alembert's principle as exposited by Kane and others [4-8], has been shown, for large systems, to possess the advantages of both Lagrange's equations and Newton's laws, but without the corresponding disadvantages. That is, the principle provides for the automatic elimination of the "non-working" internal constraint forces without introducing tedious differentiation or other similar calculations.

The objective of this report is to present several sets of data validating this cable model. This data consists of: 1) a comparison of results obtained from this model with analogous results obtained from a two-dimensional multi-link pendulum model with governing equations developed by Lagrange's equations; 2) a comparison of data from the above models with the displacement and natural frequencies of a hanging cable with data obtained analytically from a linear partial differential equation model; and 3) a comparison of model data for a submerged pendulum with experimental data recorded at the Civil Engineering Laboratory at Port Hueneme, California.

The balance of this report is divided into four parts with the following part summarizing the basic equations of the kinematics and dynamics of the cable model. This is followed by the development of the two-dimensional Lagrange multi-link pendulum model. The comparisons of the models with each other and with analytical and experimental data are presented in the next part. The final part contains some concluding remarks on the significance of the validation and on the application of the model.

THE FINITE SEGMENT MODEL

Configuration

Consider again the representation of the model as shown in Figure 1. To establish a geometrical accounting for this system, select one link (say the first link) as the reference link. Next, label or number the other links in ascending progression away from this link as shown in Figure 1. The configuration and kinematics of each body of this system may then be developed relative to the reference link which, in turn, has its configuration and kinematics defined relative to an inertial reference frame R.

Consider a typical pair of adjoining links such as L_j and L_k as shown in Figure 2. Let $j<k$, that is, let $j=k-1$. Then the general orientation of L_k relative to L_j, may be defined in terms of the relative inclination of the dextral orthogonal unit vector sets, $\underset{\sim}{n}_{ji}$ and $\underset{\sim}{n}_{ki}$ $(i=1,2,3)$ fixed in L_j and L_k, as shown in Figure 2. Specifically, let L_j and L_k be oriented so that $\underset{\sim}{n}_{ji}$ and $\underset{\sim}{n}_{ki}$ are respectively parallel. Then L_k may be brought into any given orientation relative to L_j by three successive dextral rotations about axes parallel to $\underset{\sim}{n}_{k1}$, $\underset{\sim}{n}_{k2}$, and $\underset{\sim}{n}_{k3}$ through the angles α_k, β_k, and γ_k. $\underset{\sim}{n}_{ji}$ and $\underset{\sim}{n}_{ki}$ are then related to each other as:

$$\underset{\sim}{n}_{ji} = SK_{jm}\underset{\sim}{n}_{km} \qquad (1)$$

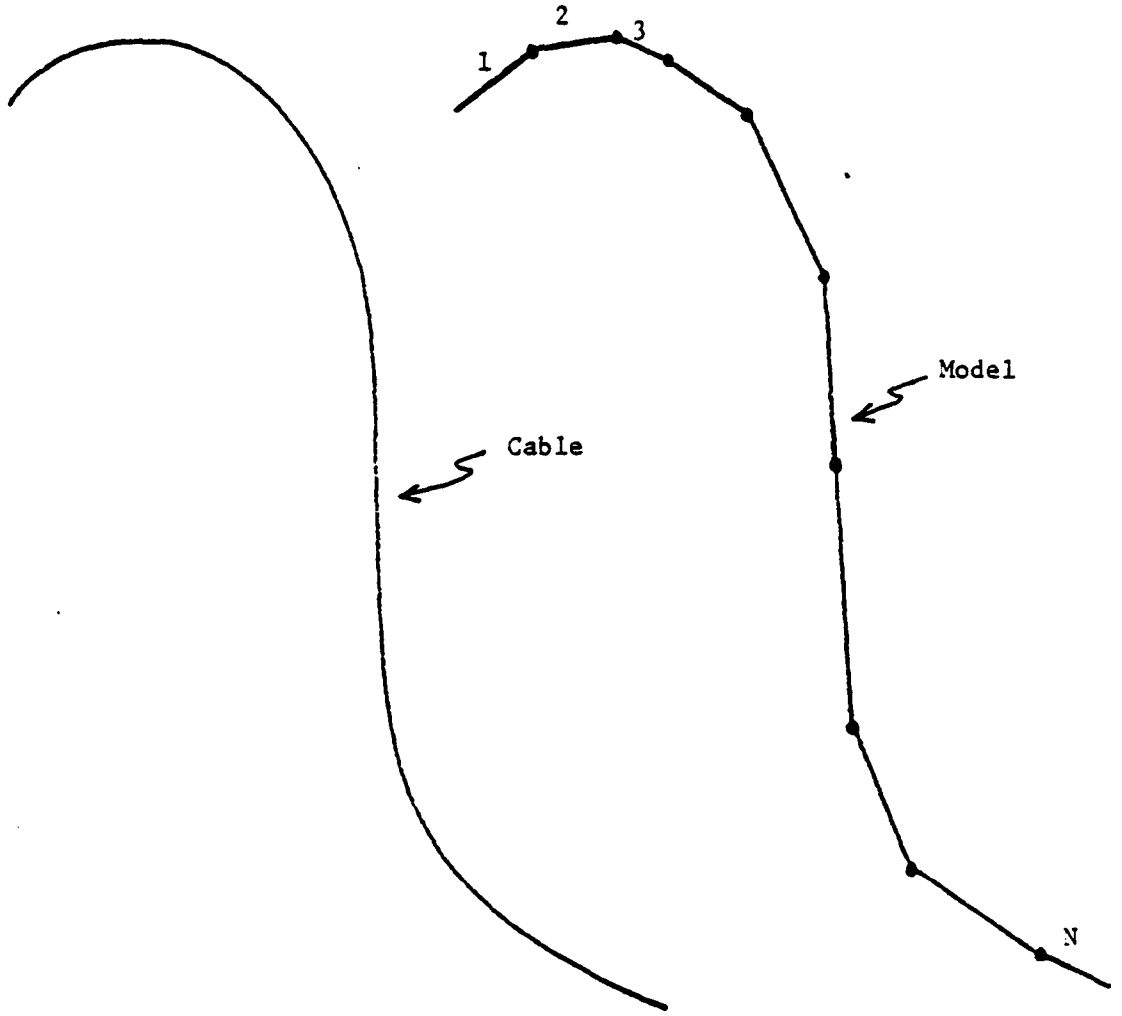

Figure 1. The Finite Segment Cable Model

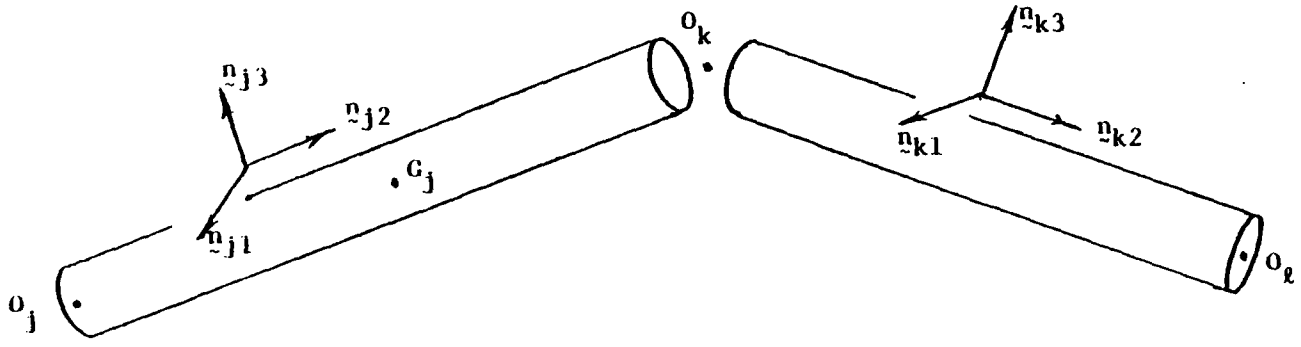

Figure 2. Two Typical Adjoining Links

where SK is a 3x3 orthogonal transformation matrix ("shifter") defined as [9]:

$$SK_{im} = \underset{\sim}{n}_{ij} \cdot \underset{\sim}{n}_{km} \tag{2}$$

(Regarding notation, repeated subscripts, such as m in the right side of Equation (1) represent a sum over the range (1,2,3) of that index.)

SK may be written as the product of three orthogonal matrices as:

$$SK = AK\ BK\ GK \tag{3}$$

where

$$AK = \begin{bmatrix} 1 & 0 & 0 \\ 0 & C\alpha_k & -S\alpha_k \\ 0 & S\alpha_k & C\alpha_k \end{bmatrix} \tag{4}$$

$$BK = \begin{bmatrix} C\beta_k & 0 & S\beta_k \\ 0 & 1 & 0 \\ -S\beta_k & 0 & C\beta_k \end{bmatrix} \tag{5}$$

$$GK = \begin{bmatrix} C\gamma_k & -S\gamma_k & 0 \\ S\gamma_k & C\gamma_k & 0 \\ 0 & 0 & 1 \end{bmatrix} \tag{6}$$

where S and C represent the sine and cosine.

These expressions allow for the transformation of components of vectors referred to one link of the system into components referred to any other link of the system, and, in particular, to the inertial reference frame R.

Since these transformation matrices play a central role throughout the analysis, it is helpful to also have an algorithm for this derivative, expecially the derivative of SOK, the transformation matrix between $\underset{\sim}{n}_{ki}$ and $\underset{\sim}{n}_{oi}$ where the $\underset{\sim}{n}_{oi}$ are fixed in R. Specifically, SOK is

$$SOK_{ij} = \underset{\sim}{n}_{oi} \cdot \underset{\sim}{n}_{kj} \tag{7}$$

Hence, since the $\underset{\sim}{n}_{oi}$ are fixed and therefore constant in R, the following is obtained:

$$d(SOK_{ij})/dt = \underset{\sim}{n}_{oi} \cdot {}^{R}d\underset{\sim}{n}_{kj}/dt \tag{8}$$

where the superscript R indicates that the derivative is computed in R. However, since $\underset{\sim}{n}_{kj}$ are fixed in L_k, their derivative may be written as $\underset{\sim}{\omega}_k \times \underset{\sim}{n}_{ki}$ where $\underset{\sim}{\omega}_k$ is the angular velocity of L_k in R. Equation (8) may then be rewritten as:

$$d(SOK_{ij})/dt = -e_{imn}\omega_{kn}\underset{\sim}{n}_{om} \cdot \underset{\sim}{n}_{kj} \tag{9}$$

or as

$$d(SOK)/dt = WK\ SOK \tag{10}$$

where WK is a matrix defined as

$$WK_{im} = -e_{imn}\omega_{kn} \tag{11}$$

where ω_{kn} are the n_{on} components of $\underset{\sim}{\omega}_k$ and e_{imn} is the standard permutation symbol [9,10]. WK is simply the matrix whose dual vector [10] is $\underset{\sim}{\omega}_k$. Equation (10) thus shows that the derivative may be computed by a simple matrix multiplication.

Finally, Figure 2. contains symbols not yet defined in the sequel. O_j (j=1,...,N) is the reference point of L_j, and it is the common point of L_j and its adjacent lower-numbered link. G_j (j=1,...,N) represents the mass center of L_j. $\underset{\sim}{r}_j$ (j=1,...,N) is the position vector of G_j relative to O_j, and $\underset{\sim}{\xi}_k$ is the position vector of O_k relative to O_j. $\underset{\sim}{r}_j$ and $\underset{\sim}{\xi}_k$ are thus fixed in L_j.

Kinematics

The system shown in Figure 1. will in general have 3N+3 degrees of freedom. These may be defined in terms of generalized coordinates X_j (j=1,...,3N+3). X_1, X_2, and X_3 represent the position coordinates of O_1 in R. The succeeding triplets of coordinates represent dextral rotations of the links relative to the respective adjacent lower links.

If the axial rotation of the links is neglected, the number of degrees of freedom can be reduced to 2N+3. This also avoids singularities which are occasionally encountered with large rotations as discussed in References [11] and [12]. When the axial rotations are neglected,

the β_k are zero for each link and the BK become identity matrices. In the following kinematic analysis, the axial rotations of the links are neglected.

The angular velocity $\underset{\sim}{\omega}_k$ of L_k in R is readily obtained from the addition formula [6]:

$$\underset{\sim}{\omega}_k = \hat{\underset{\sim}{\omega}}_1 + \hat{\underset{\sim}{\omega}}_2 + \ldots + \hat{\underset{\sim}{\omega}}_k \tag{12}$$

where $\hat{\underset{\sim}{\omega}}_k$ is the angular velocity of L_k relative to L_{k-1}. By using the transformation properties of the shifters, $\hat{\underset{\sim}{\omega}}_k$ may be written as:

$$\hat{\underset{\sim}{\omega}}_k = SOJ_{im}(\dot{\alpha}_k \delta_{mi} + \dot{\gamma}_k AK_{m3})\underset{\sim}{n}_{oi} \tag{13}$$

where δ_{mn} is Kronecker's delta symbol or the identity tensor [9,10]. Hence, by repeatedly substituting from Equation (13) into Equation (12), $\underset{\sim}{\omega}_k$ takes the form:

$$\underset{\sim}{\omega}_k = \omega_{k\ell m}\dot{X}_\ell \underset{\sim}{n}_{om} \tag{14}$$

where there is a sum from 1 to 2N+3 on ℓ and from 1 to 3 on m. From Equation (13), it is seen that the non-zero $\omega_{k\ell m}$ take one of the two forms:

$$\omega_{k\ell m} = \begin{matrix} SOJ_{ml} \\ SOJ_{mn}AK_{n3} \end{matrix} \tag{15}$$

depending upon whether X_ℓ is α_k or γ_k.

The angular acceleration $\underset{\sim}{\alpha}_k$ of L_k in R may be obtained by differentiating Equation (14). Noting that the $\underset{\sim}{n}_{om}$ are constant, this becomes:

$$\underset{\sim}{\alpha}_k = (\omega_{k\ell m}\ddot{X}_\ell + \dot{\omega}_{k\ell m}\dot{X}_\ell)\underset{\sim}{n}_{om} \tag{16}$$

where from Equation (15) the non-zero $\dot{\omega}_{k\ell m}$ take one of the two forms:

$$\dot{\omega}_{k\ell m} = \frac{\dot{SOJ}_{m1}}{\dot{SOJ}_{mn}AK_{n3} + SOJ_{mn}\dot{AK}_{n3}} \tag{17}$$

where $\dot{SOJ}$ is given by Equation (10) and where $\dot{AK}$ is obtained by differentiating Equation (4).

The velocity $\underset{\sim}{V}_j$ of G_j in R may be obtained by differentiating $\underset{\sim}{P}_j$, the position vector of G_j relative to a fixed point O in R. From Figure 1., $\underset{\sim}{P}_j$ may be expressed as:

$$\underset{\sim}{P}_j = (X_k + SOJ_{k\ell}r_{j\ell} + \sum_{M=1}^{j-1} SOM_{k\ell}\xi_{M\ell})\underset{\sim}{n}_{ok} \tag{18}$$

where, as before, there is a sum over k and ℓ from 1 to 3. Hence, $\underset{\sim}{V}_j$ may be written in the form:

$$\underset{\sim}{V}_j = V_{j\ell k}\dot{X}_\ell \underset{\sim}{n}_{ok} \tag{19}$$

where by Equations (18), (10), and (11), the non-zero $V_{j\ell k}$ are given by:

$$V_{j\ell k} = \delta_{\ell k} \qquad (j = 1,\ldots,N;\ \ell,k = 1,2,3) \tag{20}$$

and

$$V_{j\ell k} = WJ_{kp\ell} r_{jp} + \sum_{M=1}^{j-1} WM_{kp\ell} \xi_{Mp} \tag{21}$$

where $WJ_{\ell kp}$ is defined as:

$$WJ_{kp\ell} = [\partial WJ_{kq} / \partial \dot{X}_\ell] SOJ_{qp} \qquad (\ell=1,\ldots,2N+3;\ k,p=1,2,3) \tag{22}$$

Using Equation (11), $WJ_{kp\ell}$ may be written in the form:

$$WJ_{kp\ell} = -e_{kqs} \omega_{j\ell s} SOJ_{qp} \tag{23}$$

The acceleration $\underset{\sim}{a}_j$ of G_j in R may be obtained by differentiating Equation (19), leading to:

$$\underset{\sim}{a}_j = (V_{j\ell k} \ddot{X}_\ell + \dot{V}_{j\ell k} \dot{X}_\ell) \underset{\sim}{n}_{ok} \tag{24}$$

where by Equations (20) and (21), the non-zero $\dot{V}_{j\ell k}$ are given by:

$$\dot{V}_{j\ell k} = \dot{WJ}_{kp\ell} r_p^j + \sum_{M=1}^{j-1} \dot{WM}_{kp\ell} \xi_p^M \tag{25}$$

where by Equation (23) $\dot{WJ}_{kp\ell}$ is:

$$\dot{WJ}_{kp\ell} = -e_{kqs} (\dot{\omega}_{j\ell s} SOJ_{qp} + \omega_{j\ell s} \dot{SOJ}_{qp}) \tag{26}$$

Therefore, the kinematical description of the system is defined by Equations (14), (16), (19), and (24), and specifically by the four block

matrices $\omega_{j\ell k}$, $\dot{\omega}_{j\ell k}$, $V_{j\ell k}$, and $\dot{V}_{j\ell k}$. From Equations (15), (17), (21), and (25), it is seen that each of these matrices may be computed by vector and matrix multiplications which are easily developed into computer algorithms. These matrices play a central role in the development of the equations of motion of the model.

Equations of Motion

Consider again the cable model of Figure 1. Let the externally applied force system on each link L_k be replaced by an equivalent force system consisting of a single force $\underset{\sim}{F}_j$, passing through G_j together with a couple with torque $\underset{\sim}{M}_j$. Then Lagrange's form of d'Alembert's principle states that the governing dynamical equations of motion for the chain system are:

$$F_\ell + F_\ell^* = 0 \qquad (\ell = 1,\ldots,2N+3) \tag{27}$$

F_ℓ are called "generalized active forces" and they are given by:

$$F_\ell = V_{j\ell k} F_{jk} + \omega_{j\ell k} M_{jk} \tag{28}$$

where there is a sum from 1 to N on j and from 1 to 3 on k, and where F_{jk} and M_{jk} are the n_{ok} components of $\underset{\sim}{F}_j$ and $\underset{\sim}{M}_j$. F_ℓ^* are called "generalized inertia forces" and they are given by:

$$F_\ell^* = V_{j\ell k} F_{jk}^* + \omega_{j\ell k} M_{jk}^* \tag{29}$$

where the indices follow the same rules as in Equation (28) and where F^*_{jk} and M^*_{jk} are the $\underset{\sim}{n}_{ok}$ components of the inertia forces $\underset{\sim}{F}^*_j$ and inertia torques $\underset{\sim}{M}^*_j$ given by the expressions [6]:

$$\underset{\sim}{F}^*_j = -m_j \underset{\sim}{a}_j \qquad \text{(no sum)} \tag{30}$$

and

$$\underset{\sim}{M}^*_j = -\underset{\sim}{I}_j \cdot \underset{\sim}{\alpha}_j - \underset{\sim}{\omega}_j \times (\underset{\sim}{I}_j \cdot \underset{\sim}{\omega}_j) \qquad \text{(no sum)} \tag{31}$$

where m_j is the mass of L_j and $\underset{\sim}{I}_j$ is the inertia dyadic of L_j relative to G_j $(j=1,\ldots,N)$.

By substitutint Equations (16) and (24) into Equations (30) and (31) and ultimately into Equation (27), the equations of motion may be written in the form:

$$a_{\ell p}\ddot{X}_p = f_\ell \qquad (\ell = 1,\ldots,2N+3) \tag{32}$$

where there is a sum from 1 to 2N+3 on p and where $a_{\ell p}$ and f_ℓ are given by:

$$a_{\ell p} = m_j V_{jpk} V_{j\ell k} + I_{jkn} \omega_{jpn} \omega_{j\ell k} \tag{33}$$

and

$$f_\ell = -(F_\ell + m_j V_{j\ell k} \dot{V}_{jqk} \dot{X}_q + I_{jkn} \omega_{j\ell n} \dot{\omega}_{jqk} \dot{X}_q$$

$$+ e_{mnk} \omega_{jqn} \omega_{jsr} V_{j\ell k} I_{jmr} \dot{X}_q \dot{X}_s) \qquad (34)$$

where there is a sum from 1 to N on j, q, and s and a sum from 1 to 3 on the other repeated indices.

Equations (32) form a set of 2N+3 simultaneous ordinary, nonlinear differential equations determining the 2N+3 generalized coordinates X_ℓ of the cable system. Since the coefficients $a_{\ell p}$ and f_ℓ, of these equations are algebraic functions of the physical parameters, and the four arrays $V_{j\ell k}$, $\dot{V}_{j\ell k}$, $\omega_{j\ell k}$, and $\dot{\omega}_{j\ell k}$, the equations may be generated on a computer. Furthermore, once they are developed, they may also be solved numerically by a computer by using a standard numerical integration routine.

Computer Code

Numerical algorithms to evaluate the above parameters and expressions have been developed and compiled into a user-oriented computer code. As input, the code requires: the number of links; the masses; the centroidal principal inertia matrices; the mass center positions; the connection (or reference) point positions; the motion profile for those links with specified motion; the applied forces and moments; and the initial configuration.

The output of the code includes: the values of all variables and their first derivatives; the mass center positions, velocities, and accelerations; and the connection point positions, velocities, and accelerations.

LAGRANGE MULTI-LINK PENDULUM MODEL

To obtain an analytical verification of the governing equations (32), consider the two-dimensional oscillations of a multilink hanging pendulum with a concentrated end mass as shown in Figure 3. This system has N degrees of freedom which may be described by the angles $\theta_1,\ldots,\theta_N$ as shown in Figure 3. The equations of motion of this relatively simple system can be obtained through Equations (32) or independently by using Lagrange's equations.

If each link has the same mass m and length ℓ the kinetic energy K of the system may be expressed as:

$$K = (m/2)[\underline{V}_{G_1}^2 + \underline{V}_{G_2}^2 + \ldots + \underline{V}_{G_N}^2 + (\ell^2/12)(\dot{\theta}_1^2 + \dot{\theta}_2^2 + \ldots + \dot{\theta}_N^2)] + (M/2)\underline{V}_Q^2 \tag{35}$$

where the G_i $(i = 1,\ldots,N)$ are the mass centers of the links, Q is the end point with mass M. The velocity of a typical mass center G_i may be expressed as:

$$\underline{V}_{G_i} = \ell(\dot{\theta}_1\underline{n}_1 + \dot{\theta}_2\underline{n}_2 + \ldots + \dot{\theta}_i\underline{n}_i) \tag{36}$$

where the $\underline{n}_i$ $(i = 1,\ldots,N)$ are unit vectors normal to the links as shown in Figure 3. By substituting expressions of the form of Equation (36)

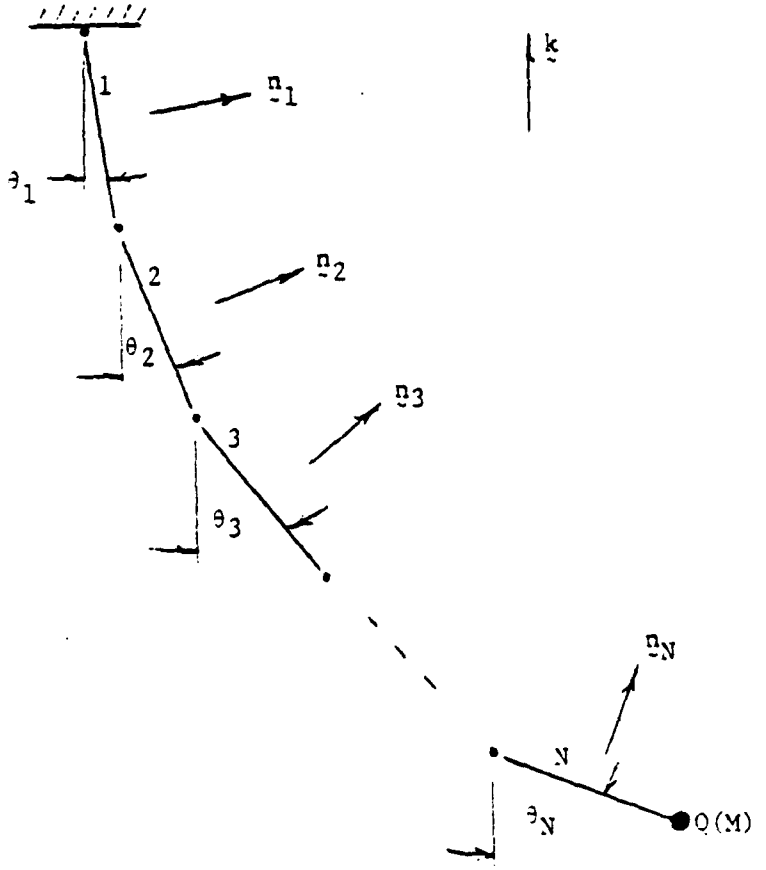

Figure 3. Two-Dimensional Multilink Pendulum Model

into Equation (35) and by carrying out the scalar products, the kinetic energy may be written in the form:

$$K = (m\ell^2/2) \sum_{i=1}^{N} \sum_{j=1}^{N} m_{ij} \dot{\theta}_i \dot{\theta}_j \tag{37}$$

where the m_{ij} are given by the expressions:

$$m_{ij} = (1/2)\,[1 + 2(N-k) + 2(M/m)]\cos(\theta_j - \theta_i) \tag{38}$$

if $i \neq j$ and k is the larger of i and j

and

$$m_{ij} = [(N - i) + (1/3) + (M/m)] \qquad \text{if } i=j \tag{39}$$

Lagrange's equations then lead to governing equations of motion of the form [6]:

$$d(\partial K/\partial \dot{\theta}_i)dt - \partial K/\partial \theta_i = F_{\theta_i} \qquad (i = 1,\ldots,N) \tag{40}$$

where F_{θ_i} is the generalized active force associated with θ_i. The only forces making a non-zero contribution to F_{θ_i} are the weight forces. Hence, F_{θ_i} may be written as:

$$F_{\theta_i} = \sum_{j=1}^{N} (\partial V_{Q_i}/\partial \dot{\theta}_j) \cdot (-mg\underset{\sim}{k}) + (\partial V_O/\partial \dot{\theta}_j) \cdot (-Mg\underset{\sim}{k}) \tag{41}$$

where $\underset{\sim}{k}$ is the vertical unit vector as shown in Figure 3. and g is the gravitational constant.

By substituting Equation (37) and (41) into Equations (40), and by carrying out the indicated operations, the equations of motion take the form:

$$\sum_{j=1}^{N} [m_{ij}\ddot{\theta}_j + p_{ij}\dot{\theta}_j^2 + (g/\ell)k_{ij}] = 0 \qquad i = 1,\ldots,N \tag{42}$$

where the m_{ij} are given in Equations (38) and (39) and where p_{ij} and k_{ij} are given by the expressions:

$$p_{ij} = (1/2)[1 + 2(N-k) + 2(M/m)]\sin(\theta_i - \theta_j) \tag{43}$$

if $i \neq j$ and k is the larger of i and j

and

$$p_{ij} = 0 \qquad \text{if } i = j \tag{44}$$

and

$$k_{ij} = 0 \qquad \text{if } i \neq j \tag{45}$$

and, finally

$$k_{ij} = [N - i + (1/2) + (M/m)]\sin\theta_i \qquad \text{if } i = j \tag{46}$$

MODEL VALIDATION AND COMPARISON

It is relatively easy to show - particularly if the number of links is small - that the equations of motion given by Equations (32) and (42) are the same. (This, of course, requires the conversion of the relative orientation angles used in Equations (32) to absolute angles as shown in Figure 3.) Hence, when Equations (32) and (42) were independently integrated for a number of cases as described below the results were identical.

The Hanging Chain

The small oscillations and natural frequencies of a hanging cable or chain have been examined and studied by several writers, including Salvadori and Schwartz [13] and Woodward [14]. These investigations involve the solution of the governing partial differential equation modelling the continuum of the hanging cable.

For an initially straight cable inclined at an angle ϑ_0 with the vertical, and released from rest, the horizontal displacement y may be expressed approximately as [13]:

$$y = y(x,t) = 8\theta_0 L[0.139J_0(2.40\sqrt{x/L})\cos 1.20\sqrt{g/L}\, t$$
$$- 0.0175\, J_0(5.52\sqrt{x/L})\cos 2.76\sqrt{g/L}\, t \qquad (47)$$
$$+ 0.00568J_0(8.65\sqrt{x/L})\cos 4.33\sqrt{g/L}\, t\,]$$

where x is the vertical coordinate along the cable, t is the time, L is the total cable length, and J_0 is the Bessel function of order zero.

For a 15 ft. cable or chain modelled by 15, 1 ft. links, Equation (32) was integrated for various θ_0 and the results were compared with those produced by Equation (47). The comparisons of the predicted shapes as the chain passes the vertical are shown in Figures 4a. and 4b.

Natural Frequencies

For small oscillations, Woodward [14] has solved the governing partial differential equation of a hanging cable with a concentrated end mass. He has calculated and tabulated the natural frequencies for various end-mass to cable-mass ratios. By linearizing Equation (42), the analogous finite segment eigenvalue problem can be solved and the results compared with those of Woodward [14]. Table I. shows a comparison of results for the lowest frequency for chains of 5, 10, and 100 links respectively. Table II. shows the same comparison for the second lowest frequency. Finally, to show the convergence of the finite segment model, Table III. presents a comparison for the fifth frequency for chains of 5, 10, 20, 50, and 100 links. (The numbers listed in these tables are $2\omega\sqrt{L/g}$ where ω is the natural frequency.)

TABLE I. A Comparison of the Finite Segment Model and a Continuum Model for the Lowest Natural Frequency for a Hanging Cable.

End-Mass/Cable-Mass Ratio m_2/m_c	Number of Links N = 5	Number of Links N = 10	Number of Links N = 100	Continuum Results [14]
0.00	2.4077	2.405	2.405	2.405
0.1	2.317	2.315	2.315	2.315
0.2	2.261	2.260	2.260	2.260
0.5	2.174	2.173	2.173	2.173
1.0	2.113	2.113	2.113	2.113
2.0	2.067	2.067	2.067	2.067
5.0	2.030	2.030	2.030	2.030
10.0	2.016	2.016	2.016	2.016
20.0	2.008	2.008	2.008	2.011
50.0	2.003	2.003	2.003	2.001

Natural Frequency: $2\omega_1\sqrt{L/g}$

TABLE II. A Comparison of the Finite Segment Model and a Continuum Model for the Second Lowest Natural Frequency for a Hanging Cable.

End-Mass/Cable-Mass Ratio M/m_c \ N	Number of Links 5	10	100	Continuum Results [14]
0.0	5.714	5.574	5.521	5.520
0.1	5.788	5.672	5.632	5.632
0.2	6.067	5.963	5.929	5.928
0.5	6.972	6.873	6.840	6.840
1.0	8.308	8.200	8.164	8.163
2.0	10.485	10.354	10.311	10.311
5.0	15.247	15.060	14.997	14.998
10.0	20.892	20.637	20.564	20.553
20.0	29.059	28.706	28.614	28.588
50.0	45.478	44.937	44.673	44.739

Natural Frequency $2\omega_2\sqrt{L/g}$

TABLE III. A Comparison of the Finite-Segment Model and a Continuum Model for the Fifth Natural Frequency for a Hanging Cable.

End-Mass/Cable-Mass Ratio M/m_c \ N	Number of Links					Continuum Results [14]
	5	10	20	50	100	
0.0	22.632	16.965	15.584	15.065	14.968	14.931
0.1	24.392	19.192	18.028	17.686	17.636	17.619
0.2	26.089	21.267	20.119	19.786	19.738	19.722
0.5	30.719	26.223	24.931	24.564	24.512	24.493
1.0	37.291	32.567	31.014	30.578	30.515	30.493
2.0	47.904	42.300	40.311	39.756	39.675	39.648
5.0	70.871	62.869	59.928	59.112	58.996	58.951
10.0	97.861	112.282	82.820	81.679	81.546	81.466
20.0	136.722	121.384	115.709	114.146	113.955	113.811
50.0	214.691	190.418	181.655	179.264	178.654	178.511

Natural Frequency $2\omega_5\sqrt{L/g}$

Submerged Catenary Cable

An experimental verification of the finite segment model can be obtained by comparison with data recorded at the U.S. Navy Civil Engineering Laboratory at Port Hueneme, California. In these experiments a totally submerged cable supported at one end, with a spherical body at the other end was initially held in a catenary shape and then released from rest [15,16]. The subsequent cable shape and motion were recorded. The same experiment was simulated using the finite segment cable model and the computer model SEADYN of Reference [15]. Table IV and Figure 5. show a comparison of the experimental and computed results for the end-body displacement. (In the analysis using Equations (32), the fluid forces were modelled by using results of References [3] and [17].)

TABLE IV. A Comparison of the Finite Segment Model, SEADYN [15,16] and Experimental Results for the End Displacement of a Submerged Cable.

Time	Experimental Results (X,Y)(ft)	SEADYN Results (X,Y)(ft)	Finite-Segment Model Results (X,Y)(ft)
0.0	20.5, 1.25	20.5, 1.25	20.5, 1.25
2.0	20.3, 6.65	20.71, 8.86	20.52, 7.97
4.0	20.2, 15.65	21.01,16.81	21.11,15.34
6.0	20.2, 24.15	21.31,22.41	21.0, 22.21
8.0	20.5, 32.65	21.07,27.47	20.89,28.97
10.0	20.5, 40.55	20.77,32.29	20.84,35.78
12.0	20.5, 46.95	20.54,37.35	20.88,42.61
14.0	20.5, 51.15	20.24,42.11	21.0, 49.19
16.0	20.0, 52.85	20.24,46.81	21.05,53.25
18.0	19.5, 53.55	19.64,51.02	20.63,54.06
20.0	18.9, 53.95	19.17,53.07	19.89,54.49

NOTE: X is the Horizontal Coordinate of the Spherical End-Body and Y is the Depth Coordinate.

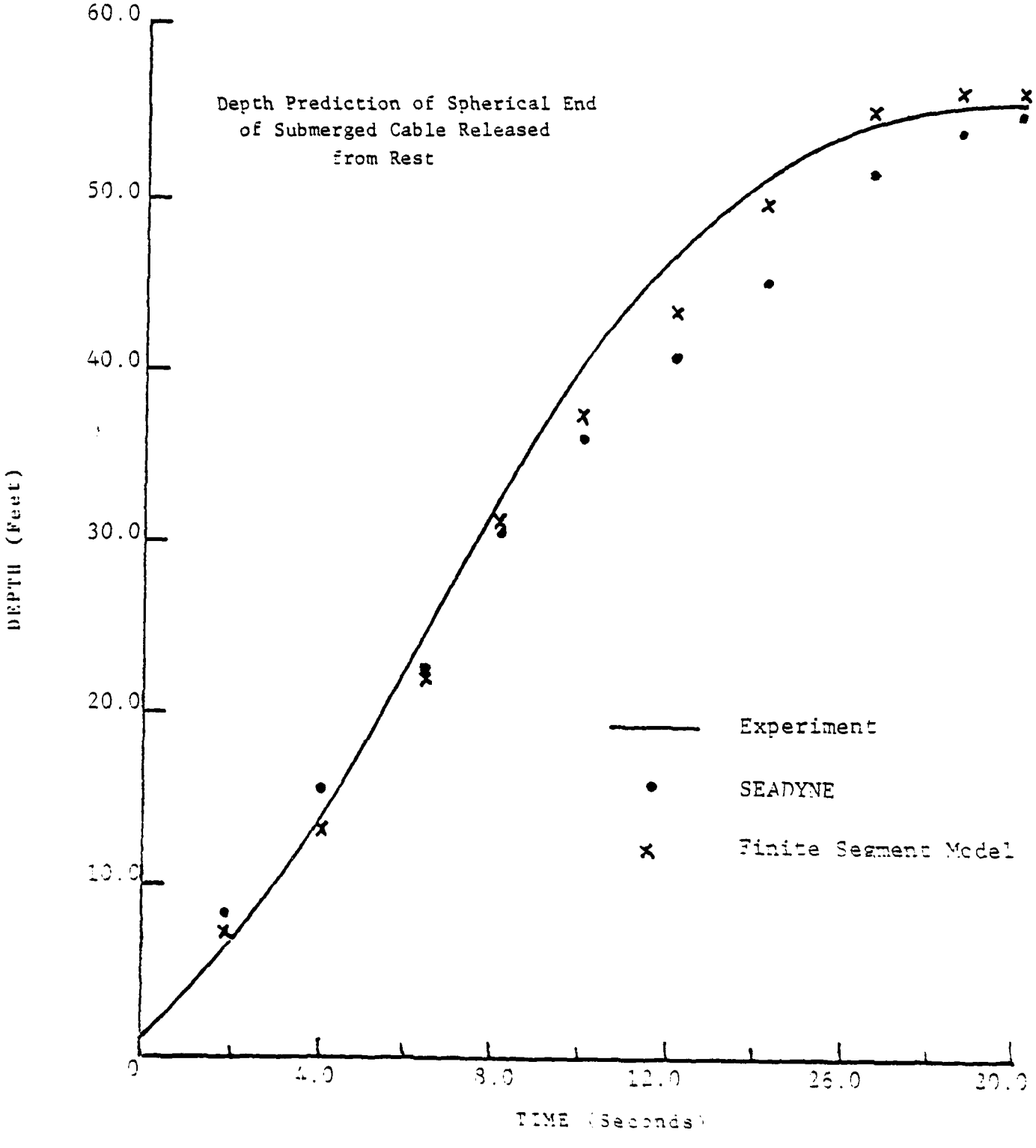

Figure 5. Comparison of Depth Predictions.

CONCLUSIONS AND APPLICATIONS

Figure 4a. shows excellent agreement between the finite segment model and the linear continuum model for small initial displacement angle. Indeed, the continuum model and the approximate solution of Equation (47) cannot be considered valid for large displacements. Figures 4a. and 4b. are thus in a sense a measure of the range of validity of the linear continuum model. Also, note that for large θ_0 the finite segment model shows the period to be larger than that predicted by the linear model. This is consistent with nonlinear pendulum theory [18].

Tables I, II and III show the convergence of the finite-segment model to the linear continuum model for small amplitude oscillations. For the lowest frequency there is excellent agreement with only five links in the finite segment model. Moreover, even for the fifth frequency there is relatively good agreement with as few as ten links.

Finally, the comparison of the finite-segment model results with experimental results also shows good agreement. This comparison validates not only the finite-segment model, but also the modelling of the fluid forces as recorded in References [3] and [17].

These results all suggest that the finite-segment cable model can provide a very effective and efficient model of the nonlinear dynamic behavior of long heavy cables. Indeed the most appropriate applications are likely to be with long submerged towing cables, mooring cables, and hoisting cables.

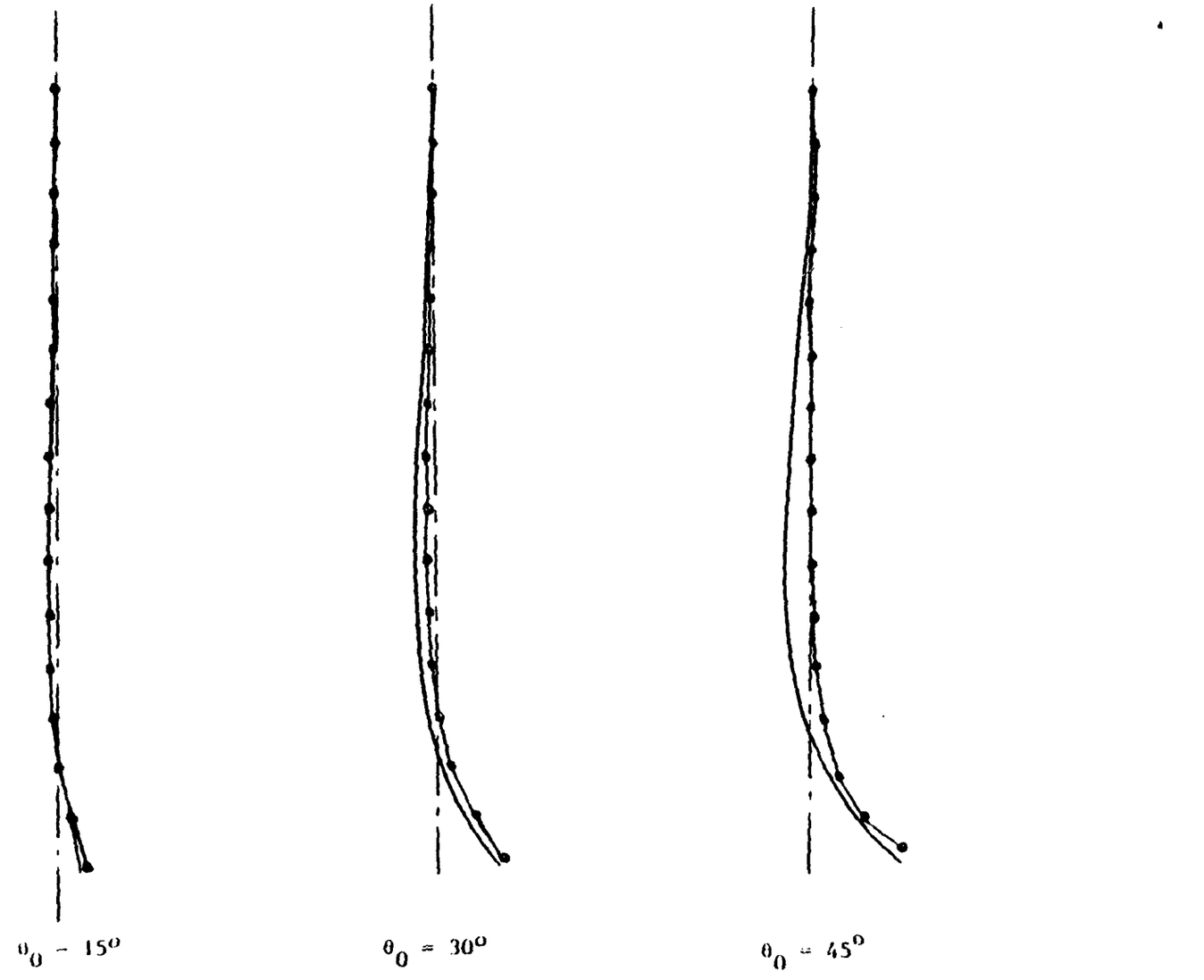

Figure 4a. Comparison of Partial Differential Equations and Cable Model Results for Initial Amplitude Angles of 15°, 30°, and 45°.

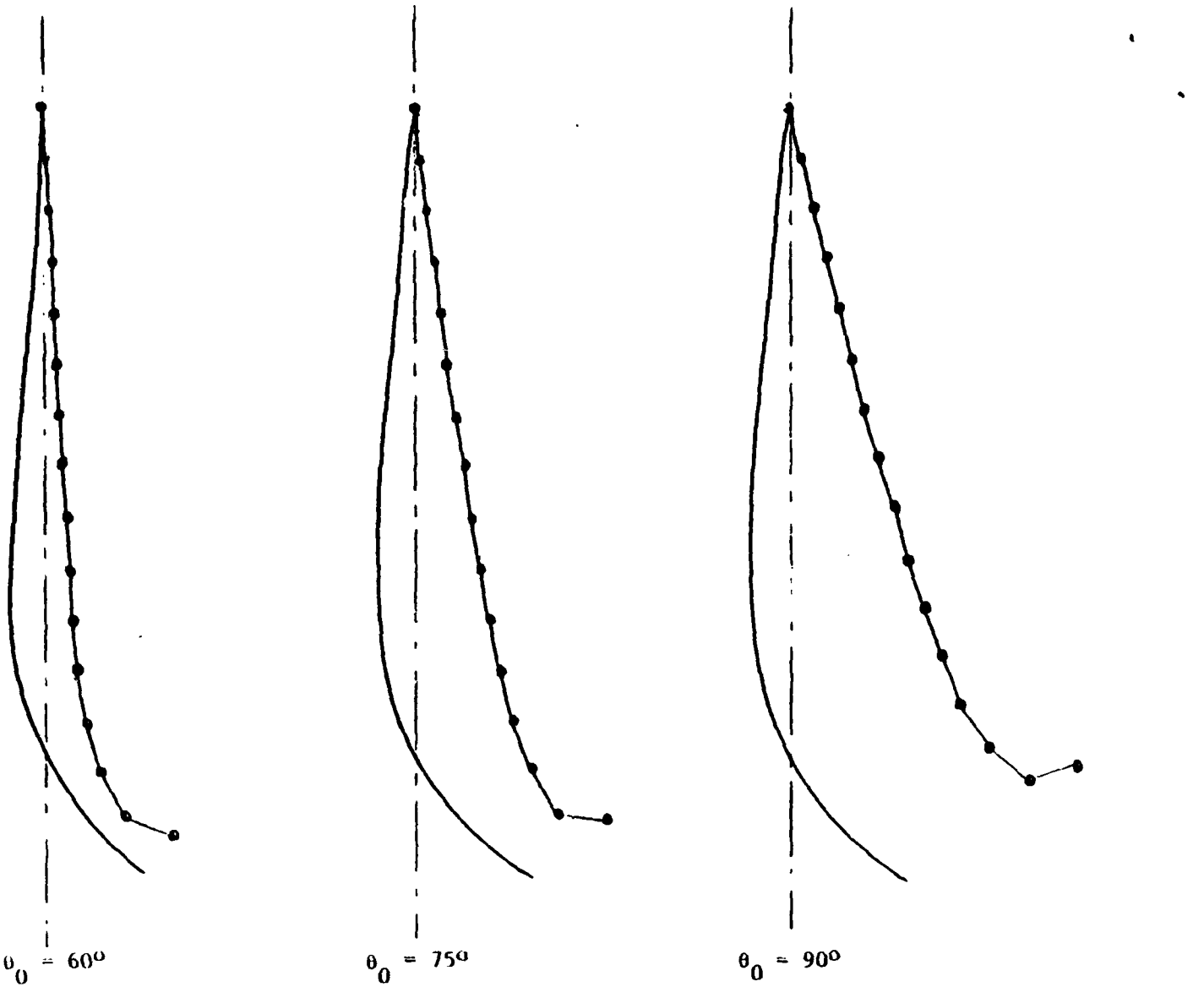

Figure 4b. Comparison of Partial Differential Equation and Cable Model Results for Initial Amplitude Angles of 60^o, 75^o, and 90^o.

REFERENCES

1. Winget, J. M., and Huston, R. L., "Cable Dynamics -- A Finite Segment Approach," Computers and Structures, Vol. 6, 1976, pp. 475-480.

2. Choo, Y., and Casarella, M. J., "A Survey of Analytical Methods for Cynamic Simulation of Cable-Body Systems," Journal of Hydronautics, Vol. 7, 1973, pp. 137-144.

3. Huston, R. L., and Kamman, J. W., "A Representation of Fluid Forces in Finite Segment Cable Models," Technical Report No. ONR-UC-MIE-090180-9, University of Cincinnati, 1980.

4. Kane, T. R., "Dynamics of Nonholonomic Systems," Journal of Applied Mechanics, Vol. 28, 1961, pp. 574-578.

5. Kane, T. R., and Wang, C. F., "On the Derivation of Equations of Motion," Journal of the Society of Industrial and Applied Mathematics, Vol. 13, 1965, pp. 487-492.

6. Kane, T. R., Dynamics, Holt, Rinehart & Winston, 1968.

7. Huston, R. L., and Passerello, C. E., "On Lagrange's Form of d'Alembert's Principle," Matrix and Tensor Quarterly, Vol. 23, 1973, pp. 109-112.

8. Kane, T. R., and Levinson, D. A., "Formulation of Equations of Motion for Complex Spacecraft," Journal of Guidance and Control, Vol. 3, No. 2, March-April, 1980, pp. 99-112.

9. Eringen, A. C., Nonlinear Theory of Continuous Media, McGraw Hill, New York, 1968.

10. Brand, L., Vector and Tensor Analysis, Wiley, New York, 1947.

11. Huston, R. L., and Passerello, C. E., "Eliminating Singularities in Governing Equations of Mechanical Systems," Mechanics Research Communications, Vol. 3, 1976, pp. 361-365.

12. Huston, R. L., Passerello, C. E., and Harlow, M. W., "Dynamics of Multi-rigid-Body Systems," Journal of Applied Mechanics, Vol. 45, No. 4, 1978, pp. 889-894.

13. Salvadori, M. G., and Schwartz, R. J., Differential Equations in Engineering Problems, Prentice Hall, New York, 1954, pp. 401-408.

14. Woodward, J. H., "Frequencies of a Hanging Chain Supporting an End Mass," The Journal of the Acoustical Society of America, Vol. 49, No. 5 (Part 2), 1971, pp. 1675-1677.

15. Palo, P. A., "Comparisons Between Small-Scale Cable Dynamics, Experimental Results and Simulation Using SEADYN and SNA PL6 Computer Models," Civil Engineering Laboratory, Naval Construction Battalion Center, Port Hueneme, CA, Report No. TM44-79-5, January 1979.

16. Dillon, D. B., "Mooring Dynamics: Computer Models and Experiments at a Sixty Foot Scale," Civil Engineering Laboratory, Naval Construction Battalion Center, Port Hueneme, CA, Report TR 4999-0004, July 1980.

17. Webster, R. L., "An Application of the Finite Element Method to the Determination of Nonlinear Static and Dynamic Responses of Underwater Cable Structures," General Electric Technical Information Series Report No. R76EMH2, Syracuse, NY, 1976.

18. Stoker, J. J. Nonlinear Vibrations, Interscience, New York, 1957, p. 25.